ELSEVIER

Contents lists available at ScienceDirect

### Journal of Power Sources

journal homepage: www.elsevier.com/locate/jpowsour



# Temperature dependent ageing mechanisms in Lithium-ion batteries — A Post-Mortem study



Thomas Waldmann\*, Marcel Wilka, Michael Kasper, Meike Fleischhammer, Margret Wohlfahrt-Mehrens

ZSW - Zentrum für Sonnenenergie- und Wasserstoff-Forschung, Baden-Württemberg, Helmholtzstrasse 8, D-89081 Ulm, Germany

#### HIGHLIGHTS

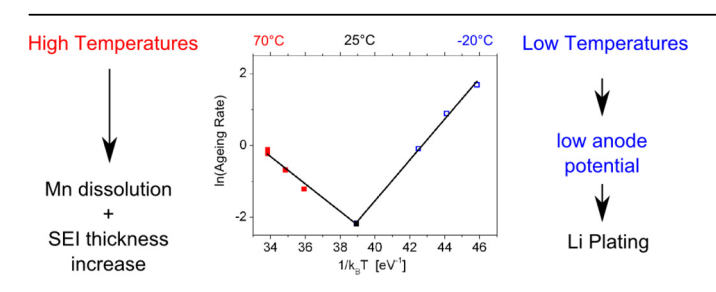
- The ageing behaviour of cycled cells is tested in the range of  $-20~^{\circ}\text{C}$  to  $+70~^{\circ}\text{C}$ .
- Temperature dependent ageing mechanisms are found by an Arrhenius plot.
- The different ageing mechanisms are proven by Post-Mortem analysis.
- The reason for the different mechanisms is found by tests with reference electrodes.

#### ARTICLE INFO

Article history:
Received 18 November 2013
Received in revised form
7 March 2014
Accepted 24 March 2014
Available online 31 March 2014

Keywords:
High-power Lithium-ion batteries
Ageing mechanisms
Electrode polarization
Arrhenius
Post-Mortem analysis
Battery life-time

#### G R A P H I C A L A B S T R A C T



#### ABSTRACT

The effects of temperatures in the range of  $-20\,^{\circ}\text{C}$  to  $70\,^{\circ}\text{C}$  on the ageing behaviour of cycled Lithium-ion batteries are investigated quantitatively by electrochemical methods and Post-Mortem analysis. Commercial 18650-type high-power cells with a Li<sub>x</sub>Ni<sub>1/3</sub>Mn<sub>1/3</sub>Co<sub>1/3</sub>O<sub>2</sub>/Li<sub>y</sub>Mn<sub>2</sub>O<sub>4</sub> blend cathode and graphite/ carbon anode were used as test system. The cells were cycled at a rate of 1 C until the discharge capacity falls below 80% of the initial capacity. Interestingly, an Arrhenius plot indicates two different ageing mechanisms for the ranges of  $-20\,^{\circ}\text{C}$  to  $25\,^{\circ}\text{C}$  and  $25\,^{\circ}\text{C}$  to  $70\,^{\circ}\text{C}$ . Below  $25\,^{\circ}\text{C}$ , the ageing rates increase with decreasing temperature, while above  $25\,^{\circ}\text{C}$  ageing is accelerated with increasing temperature. The aged 18650 cells are inspected via scanning electron microscopy (SEM), energy dispersive X-ray analysis (EDX), inductively coupled plasma (ICP), measurements of electrode thickness and X-ray diffraction (XRD) after disassembly to learn more about the chemical reasons of the degradation. The effect of different temperatures on the electrode polarizations are evaluated by assembling electrodes in pouch cells with reference electrode as a model system. We find that the dominating ageing mechanism for  $T < 25\,^{\circ}\text{C}$  is Lithium plating, while for  $T > 25\,^{\circ}\text{C}$  the cathodes show degeneration and the anodes will be increasingly covered by SEI layers.

© 2014 Elsevier B.V. All rights reserved.

#### 1. Introduction

Besides the use of Lithium-ion batteries in portable devices, they are regarded as the key technology for the next generation of

vehicles [1–3] and nearly all car manufacturers have already introduced one or more vehicles that utilize electric drive systems. Apart from major advantages of this technology, such as local zero emission vehicles and independence from the oil market, there are still problems regarding the life-time of car batteries. In order to improve the long-term usability of Lithium-ion batteries, it is essential to gather more knowledge about the chemical processes that contribute to battery ageing. The state-of-health (SOH) which

<sup>\*</sup> Corresponding author. Tel.: +49 (0)731 9530 212; fax: +49 (0)731 9530 666. E-mail address: thomas.waldmann@zsw-bw.de (T. Waldmann).

determines the 'age' of a battery is commonly defined as the discharge capacity of an aged cell compared to the discharge capacity of the same cell when it was new. An SOH < 80% is commonly regarded as end-of-life (EOL) criterion for a battery. The course of SOH as function of time during the ageing process is influenced by the conditions of operation of the battery and contains information on the ageing rate of the cell if the experimental conditions are well-defined. Such defined model conditions can for example be achieved by cycling at defined temperatures [4]. In order to learn more about ageing processes on the microscopic scale, there have been several studies regarding the ageing of electrodes [5,6], electrolyte [7–9] and separator materials [10] as well as the electrode | electrolyte interface [11-15]. Known ageing effects comprise Mn dissolution from the cathode [16–19] and subsequent deposition on the anode [5], Mn re-deposition on the cathode [20], particle cracks [21], loss of cyclable Li [22–24], Lithium plating [25,25–28] or solid-electrolyte interface (SEI) growth [13-15,24,27]. It was also shown that variations of the material composition can lead to improved batteries, e.g. by using additives [29,30] or blending of cathode materials [31–33]. Since it may take several years to reach the EOL criterion of a battery under moderate operation conditions, accelerated ageing tests are used. In such tests the batteries are put under stress for example by elevated temperatures [4,34–37], however, there is a lack of data on the ageing induced by low temperatures. The speed of ageing can quantitatively be described by ageing rates, which are contained in the capacity fade curves. After measuring ageing rates as a function of temperature, it is common practice to linearize the data by plotting ln(r) vs. 1/T, which is known as Arrhenius plot [38,39] according to the equation

$$r = A \exp\left(-\frac{E_{\rm a}}{k_{\rm B}T}\right) \tag{1}$$

with the ageing rate r, the pre-exponential factor A, the activation barrier  $E_a$  and the Boltzmann constant  $k_B$ . Arrhenius theory has been used in the field of Lithium-ion batteries to determine activation barriers for ageing [36,40] and other processes [41-44]. However, it is often disregarded that the linear Arrhenius-like behaviour is only valid in certain temperature intervals. A change of the slope in an Arrhenius plot is an indication for a mechanism change [38]. Arrhenius behaviour has been observed for Lithiumion batteries [14,36,45], but not over the whole temperature range which a battery electric car might be exposed to (-20 to)70 °C). In literature, ageing measurements are carried out mostly below 60 °C, since changes in the reaction mechanism are expected [4]. Only few authors performed tests at 65 °C [4], 70 °C [46] or 85 °C [47]. It depends on the battery chemistry and design at which temperature a change of the ageing mechanism occurs. Results on 18650 cells with  $Li_xNi_{1/3}Mn_{1/3}Co_{1/3}O_2/Li_vMn_2O_4$  blend cathodes have been published before, however, different ageing conditions and electrochemical instead of Post-Mortem analysis was applied [24.27.48].

In this paper, we use temperatures in the range of  $-20\,^{\circ}\mathrm{C}$  to  $70\,^{\circ}\mathrm{C}$  to accelerate the ageing of 18650 cells with blend cathodes under cycling conditions. By utilizing an Arrhenius plot, we find two different ageing mechanisms depending on the ageing temperature. The chemical reasons for the degradation mechanisms are identified by Post-Mortem analysis of the 18650 cells and by polarization measurements with pouch cells with reference electrode.

#### 2. Experimental

The investigated commercial batteries used in this work have an initial capacity of 1.5 Ah and contain Li<sub>x</sub>Ni<sub>1/3</sub>Mn<sub>1/3</sub>Co<sub>1/3</sub>O<sub>2</sub>/Li<sub>y</sub>Mn<sub>2</sub>O<sub>4</sub>

blend cathodes and graphite/carbon anodes. All tested cells in the present study were very similar in mass, open circuit voltage, internal resistance and capacity at SOH = 100%, qualifying them for systematic ageing tests [48]. To compensate the small variations in the capacities and internal resistances of the new batteries, both values are relating to those of the respective un-aged batteries and are specified in %. The cells were aged inside climate chambers (Vötsch) and electrochemical measurements were conducted using a Basytec CTS system. All charging procedures during cycling and capacity tests were done using a constant current/constant voltage (CCCV) test protocol, while the discharge was conducted with constant current (CC). The cycled cells were charged and discharged between 2.0 V and 4.2 V with 1.5 A (1 C) in all cases. The stop criterion for all ageing tests was SOH = 80% with respect to discharging at a rate of 1 C at 25 °C. At different points in time during the ageing tests, the tests were interrupted for capacity tests (see Fig. 2). For comparability reasons, the cells were allowed to relax to 25 °C and capacities were measured at a rate of 1 C. Subsequently, the ageing tests were continued, if the EOL criterion was not fulfilled. Ageing rates were determined tangential from the slope SOH(t) vs. t plots with the intercept point SOH(t = 0) = 100%. Before the disassembly by a high precision saw, the 18650 cells were discharged to their end-of-discharge voltage of 2.0 V, to keep both, risk and corrosion issues low. The electrodes were separated and washed with DMC by using a self developed washing procedure until the remaining conductive salt concentration was reduced to a no more analytically significant value. The electrode samples taken from the outer part of the jelly rolls were analyzed by SEM/EDX (LEO 1530VP Gemini), ICP and XRD. The X-ray diffraction was performed with a Siemens D5000 (CuKa radiation in reflection geometry). The lattice parameters were refined by means of the whole-powder pattern decomposition (WPPD) method (Pawley) using TOPAS (Bruker). Polarization values were calculated with respect to the second cycle at 25 °C and 1 C.

#### 3. Results and discussion

#### 3.1. Un-aged commercial 18650 cells

First, the un-aged 18650 batteries were characterized, in order to compare the results with those from the aged cells. ICP measurements showed a 1:1 ratio for the Li<sub>x</sub>Ni<sub>1/3</sub>Mn<sub>1/3</sub>Co<sub>1/3</sub>O<sub>2</sub>:Li<sub>y</sub>Mn<sub>2</sub>O<sub>4</sub> blend. The chemical composition of single particles Li<sub>x</sub>Ni<sub>1/3</sub>Mn<sub>1/3</sub>Co<sub>1/3</sub>O<sub>2</sub> was determined by EDX point spectra to be 1:1:1 under consideration of the excitation radius and within the error bars. The anode consists of spherical graphite and carbon particles (Fig. 1a). For the anode material, the blend ratio is not accessible with our methods. ICP did not show significant amounts of Mn on the new anodes. The X-ray diffraction patterns of the un-aged cathodes show reflections corresponding to the layer structure *R*-3*m* (hexagonal setting) and the spinel structure (*Fd*-3*m*). XRD of un-aged cathodes revealed the lattice constants a(NMC) = 2.857703(255) Å, c(NMC) = 14.24968(245) for Li<sub>x</sub>Ni<sub>1/3</sub>Mn<sub>1/3</sub>Co<sub>1/3</sub>O<sub>2</sub> and  $a(Li_yMn_2O_4) = 8.21033(95)$  Å for Li<sub>y</sub>Mn<sub>2</sub>O<sub>4</sub>.

### 3.2. Arrhenius behaviours of capacity fade in different temperature ranges

18650 cells were cycled with charge and discharge rates of 1 C at constant temperatures between  $-20\,^{\circ}\text{C}$  and  $70\,^{\circ}\text{C}$ . As can be seen in Fig. 2, SOH(t) is a nearly linear function in the SOH range of 100%–90%, as indicated by  $R^2$ -values larger than 0.97, except for  $T=25\,^{\circ}\text{C}$  where  $R^2=0.93$ . For cycling at 1 C at 25  $^{\circ}\text{C}$ , the curve shape of the SOH(t) data in Fig. 2 is similar to the data reported by Dubarry et al., who cycled NMC/LMO blend cells at a rate of 2 C [24]. Comparing

#### Download English Version:

## https://daneshyari.com/en/article/7736626

Download Persian Version:

https://daneshyari.com/article/7736626

<u>Daneshyari.com</u>